

Development of time resolved X-ray spectroscopy in high intensity laser-plasma interactions

M. Notley, B. Fell, J. Jeffries and G. Gregori

Central Laser Facility, CCLRC Rutherford Appleton Laboratory, Chilton, Didcot, Oxon., OX11 0QX, UK

R. L. Weber and R. R. Freeman

The Ohio State University, 191 West Woodruff Ave. Columbus, OH 43210, USA

A. J. Mackinnon, R. Dickson and D. S. Hey

Lawrence Livermore National Laboratory, PO Box 808, Livermore, CA 94551, USA

F. Y. Khattak and E. Garcia-Saiz

Dept of Mathematics and Physics, Queen's University of Belfast, Belfast, BT7 1NN, UK

Main contact email address M.Notley@rl.ac.uk

Introduction

X-ray spectroscopy is a technique that has been often applied to investigate radiation transport in warm dense matter (WDM) resulting from high intensity laser matter interaction experiments^[1-4]. Such dense matter states are also found to be strongly coupled (i.e., with the Coulomb interaction among charged particles being dominant over their kinetic energy) and in highly transient regimes. This poses severe limits in the microscopic modelling of such systems as the usual plasma expansion methods are not applicable^[5].

On the other hand, the understanding of recombination dynamics, electron transport and phase transitions in WDM regimes is important for both the modelling of extreme astrophysical environments (such as the interior of white dwarfs and neutron star atmospheres) and for the success of inertial confinement fusion (ICF)^[6,7]. In this respect, the possibility of obtaining time resolved measurements is critical in such transient states. In the past, time resolved measurements at laser illuminations in the 100 TW to 1 PW regimes have been often limited by the large background (i.e., bremsstrahlung) noise generated during the interaction.

In this report, we present a novel instrument design which consists of a highly oriented pyrolytic graphite (HOPG) mosaic crystal coupled to a picosecond x-ray streak camera. We will show that by combining a highly reflective HOPG crystal in a Von-Hamos configuration^[8], good signal-to-noise ratio can be achieved in time-resolved x-ray measurements resulting from high intensity laser-plasma experiments.

Experimental Setup

The experiments were carried out at the 100 TW Vulcan laser facility at the Rutherford Appleton Laboratory (UK) using either laser pulses at 1053 nm 1.5 ps duration, or at 527 nm with 1 ns pulse duration. These pulses were focused to 10 μm (with intensity on target $I \sim 10^{18}$ W/cm²) and 100 μm , ($I \sim 10^{15}$ W/cm²) respectively, to irradiate 1 mm \times 1 mm bare Ti or sandwiched Al/Ti/Al (2 μm thick Al and 5 μm thick Ti) foil targets. The layout of the experiment is shown in Fig 1.

The dispersive element of the spectrometer is ZYA grade HOPG crystal (50 mm \times 25 mm) used in mosaic focusing mode. It was configured in a Von Hamos geometry with 115 mm radius of curvature along the sagittal axis (i.e.,

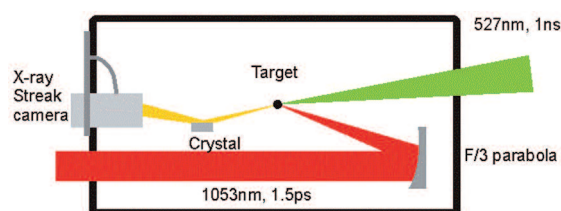


Figure 1. Experiment layout. A 1 ns pulse at 527 nm is focused to 100 μm using an F/10 lens with a random phase plate, and a 1.5 ps pulse at 1053 nm is focused to 10 μm using an F/3 parabola onto a thin foil target.

the minor axis). This was coupled with a Kentech x-ray streak camera using a CsI fluffy photocathode on a 1 μm CH substrate flash coated with Al. Fig 2 shows the set-up of the elements of the instrument. Adjustable lateral and transverse positions of the crystal relative to the target are available and determined by radius of curvature and centre wavelength of interest. A separate pumping system was designed to allow the streak camera to be kept at 10^{-6} mbar independently from the main target chamber. Beryllium, 1 mm thick, 50 mm dia. was used for the vacuum x-ray window. A 50:40 intensifier was coupled to the output phosphor of the streak camera and detection made via an 8 bit CCD capture system. The overall magnification of this system was 0.96 from input slit to output on the intensifier.

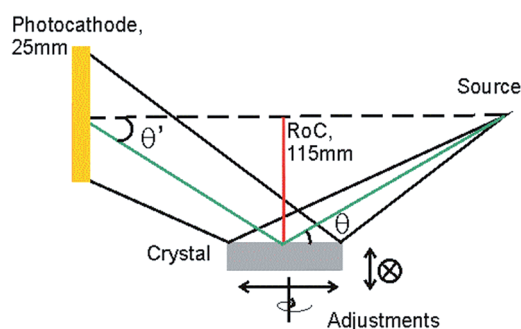


Figure 2. Spectrometer Schematic. The crystal is curved sagittally producing a line focus parallel to its surface. Detection is carried out perpendicular to this plane via x-ray streak camera, the initial detection point being the photocathode. The crystal can be adjusted to suit wavelength detection range. Source to cathode distance was 542 mm.

The spectrometer was designed to cover both the K- α (4.5 keV) and He- α lines (4.75 keV) of titanium. At $E_0=4.8$ keV, the optimal source-to-crystal distance is $F=R/\sin\theta=298$ mm, where $R=115$ mm is the radius of curvature and $\theta=22.7^\circ$ is the Bragg angle. The energy dispersion at the photocathode is thus^[9].

$$\frac{\Delta E}{\Delta x} = \frac{E_0 \cos \theta}{2F \sin \theta} \cdot \cos \theta', \quad (1)$$

which corresponds to ~ 19.7 eV/mm with a bandwidth of ~ 500 eV. Here, $\theta'=\theta$ is the angle between the photocathode normal and the diffracted x-ray from the crystal. The spectral resolution depends both on the mosaic spread of the HOPG crystal and the geometric aberrations produced by the Von-Hamos focussing. This is estimated to be ~ 7.7 eV for Ti at 4.8 keV^[8]. Source broadening is < 2 eV for a 100 μm spot size. The time response of the fluffy CsI cathode can be estimated from Henke *et al.*^[10]

$$\Delta t_{pc} = 3.37 \frac{D^2}{\varepsilon_0} \left(1 + \frac{1}{4} \left(\frac{L}{S} - 2 \right) \left(\frac{D}{V_0} \right)^2 \right), \quad (2)$$

where D is the energy spread (in eV) of the secondary electrons emitted from the cathode, V_0 is the potential between mesh and cathode (4.1 kV) in the streak camera, S the physical spacing between them (2 mm) and L the length from mesh to the phosphor (300 mm). $\varepsilon_0=V_0/S$ (in kV/mm). The deposited CsI layer was 5-10 μm thick which corresponds to an energy spread of $D\sim 1.7\text{eV}$ ^[10]. This gives $\Delta t_{pc}\sim 50\text{-}60$ ps. This number is much larger than the time response of the HOPG crystal which is related to the time difference between rays diffracted at various depths in the crystal. This time is in the order of^[11].

$$\Delta t_c = \frac{2t_e}{c \sin \theta_b}, \quad (3)$$

where t_e is the extinction depth (200 μm for carbon) and c is the speed of light. This gives $\Delta t_{pc}\sim 3$ ps. While a time resolution of ~ 50 ps is not sufficient to resolve the initial fast dynamics associated to a short-pulse laser illumination (\sim a few ps), the emission from the exploding foil and the recombining plasma develops on much longer time scales and it can still be observed. For the majority of data the streak camera was run on a time window of ~ 1.9 ns (47.5 ps/mm on the phosphor) so the fastest event visible would equate to $\sim 1\text{-}1.5$ mm on the CCD. Clearly, higher time resolutions could have been achieved by using different photocathode materials^[10]. On the other hand, fluffy CsI provides the highest x-ray sensitivity in the region of interest, and it is thus preferable for weaker signals and for studies of the recombination dynamics at late times.

Results

Streaked images of the x-ray emission from both bare and sandwiched Ti foils, in the region between 4.4 and 5.0 keV, are shown in Fig. 3. For the case of short-pulse illumination (Fig. 3a), Ti K- α emission is clearly visible for about 250 ps after the start of the pulse. On the other hand, in the case of a long pulse illumination on the same target (see Fig. 3b), the only significant emission comes from the He- α line and satellites. This starts about ~ 0.7 ns

after the beginning of the laser drive, indicating the time spent to burn through the Al layer^[12]. Indeed, in the case of bare a Ti foil (Fig. 3c), the He- α emission starts immediately at the beginning of the drive pulse.

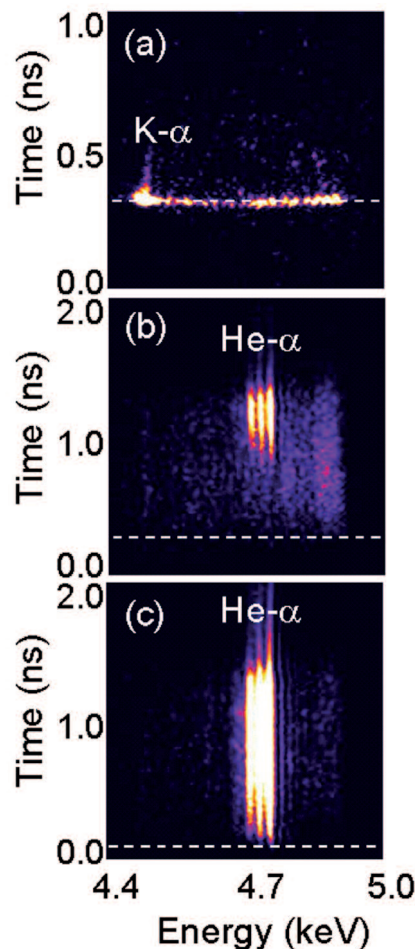


Figure 3. Experimental results. a) Streak image obtained from a 1×1 mm layered Al/Ti/Al foil target illuminated with 125 J with 1.5 ps pulse at 1053 nm; b) same target as before illuminated using 50 J with 1 ns pulse at 527 nm; c) bare 5 mm thick Ti foil illuminated at 60 J with a 1 ns pulse at 527 nm. For all cases, the streak camera was filtered with a 25 μm Al foil plus a 26 μm mylar foil in addition to the 1 mm Be window. The dotted lines indicate the start of the laser pulse ($t=0$).

Inhomogeneities in the CsI photocathode are clearly visible at the highest streak speed (Fig. 3a) as well as at lower sweep speeds and they appear as weak features on the blue side of the He- α line. This results from a non-uniform deposition of the CsI on the CH substrate. Despite such effects, the K- α emission line remains prominent. We notice that the width of the K- α line decreases with time suggesting a lower contribution from open shell transitions (i.e., from partially ionized Ti atoms) and active recombination. The separation between the Ti He- α 2p¹P resonance (at 4.75 keV) and the 2p³P (at 4.73 keV) is, from Fig. 3b-c, 1.2 mm, giving a dispersion of 20.5 eV/mm in good agreement with the theoretical value. The full width at half maximum of the 2p¹P line is ~ 8.8 eV, in agreement with previously estimated. It is also interesting to observe that in Fig. 3b-c the ratio between the primary Ti He- α 2p¹P line and the satellites is changing with time, possibly as a result of a change in temperature of the emitting plasma.

Conclusions

We have measured temporally resolved x-ray spectra in the region from 4.4 to 5.0 keV from Ti foils illuminated with intense laser pulses at the 100 TW Vulcan laser facility. These results have been obtained by coupling a high efficiency Bragg crystal to a picosecond streak camera. In order to maximize the x-ray throughput, the HOPG crystal was curved in a Von-Hamos geometry. Additional increase in sensitivity was obtained by using a CsI photocathode. We have shown that the temporal resolution of the photocathode is sufficient to observe late time K- α emission which was observed to last for about 250 ps after the start of the laser pulse. Our results indicate that this diagnostic can be used to study recombination dynamics, electron transport and phase transitions in WDM and for conditions relevant to ICF research.

This work was partially funded by the US DOE by the University of California Lawrence Livermore National Laboratory under contract no. W-7405-ENG-48 and by the US Office of Fusion Energy Science.

References

1. P. Audebert *et al.*, *Phys. Rev. Lett.*, **94**, 025004, (2005)
2. K. Eidmann, A. Saemann, U. Andiel, I. E. Golovkin, R. C. Mancini, E. Andersson and E. Förster, *J. Quant. Spectrosc. Radiat. Transfer*, **65**, 173 (2000)
3. S. B. Hansen *et al.*, *Phys. Rev. E*, **72**, 036408-1 (2005)
4. G. Gregori *et al.*, *Contrib. Plasma Phys.* **45**, 284 (2005)
5. S. Ichimaru, *Basic Principles of Plasma Physics*, Addison, Reading, MA, 1973
6. J. D. Lindl, *Inertial Confinement Fusion*, Springer-Verlag, New York, (1998)
7. R. W. Lee *et al.*, *J. Opt. Soc. Am. B*, **20**, 770, (2003)
8. G. E. Ice and C. J. Sparks, *Nucl. Instrum. Methods Phys. Res. A*, **291**, 110, (1990)
9. A. Pak, G. Gregori, J. Knight, K. Campbell, D. Price, B. Hammel, O. L. Landen and S. H. Glenzer, *Rev. Sci. Instrum.*, **75**, 3747, 2004
10. B. L. Henke, J. P. Knauer and K. Premaratne, *J. Appl. Phys.*, **52**(3), 1509, (1981)
11. T. Missalla, I. Uschmann, E. Förster, G. Jenke and D. Von der Linde, *Rev. Sci. Instrum.*, **70**, 1288, (1999)
12. M. H. Key, W. T. Toner, T. J. Goldsack, J. D. Kilkenny, S. A. Veats, P. F. Cunningham and C. L. S. Lewis, *Phys. Fluids*, **26**, 2011, (1983)